3D Modeling from AFM Measurements

Timothée Jost[*], Heinz Hügli

Institute of Microtechnology, University of Neuchâtel,
CH-2000 Neuchâtel, Switzerland

ABSTRACT

There exist many techniques for the measurement of micro and nano surfaces and also several conventional ways to represent the resulting data, such as pseudo color or isometric 3D. This paper addresses the problem of building complete 3D micro-object models from measurements in the submicrometric range. More specifically, it considers measurements provided by an atomic-force microscope (AFM) and investigates their possible use for the modeling of small 3D objects. The general approach for building complete virtual models requires to measure and merge several data sets representing the considered object observed under different orientations, or views. A straightforward application of this scheme fails when acquisition methods for micro-objects, due to physical constraints, cannot provide the required positioning information for aligning the different views. The presented approach proposes to use an a posteriori software registration procedure that aligns views by registering common overlapping parts. It relies on the sole intrinsic properties of the object geometry and does not require additional measurements The actual registration process proceeds in two steps: a first rough interactive alignment of the views, followed by their automatic matching. Such generated 3D models offer new possibilities for the analysis of micro-objects by visualization or measurement in 3D space. First experiments are presented which demonstrate, among others, the successful alignment of three AFM views of a Ni-polymer substrate (used to fix particles) by geometric matching. The final goal of this work is to build complete virtual models of submicroscopic objects, for instance quartz particles measuring about 1-3 µm.

Keywords: atomic-force microscope, AFM imaging, micro-object, 3D virtual modeling, surface registration

1. INTRODUCTION

Atomic-force microscopes (AFMs) measure surface geometry. The tip-to-sample distance information is scanned all over a defined area, providing a depth map which consists of a bidimensional array of height z measurements defined at various discrete x, y positions. Traditionally, one of the most basic ways of representing these data for viewing is using a pseudo color representation, creating an image whose pixels color vary with the z value. Using pseudo color helps to give an idea of the measured object shape.

Another means is to use a shaded view of the depth map, which is much more natural and meaningful, especially in view of the widely varying depth to length ratio (z/x or z/y) of typical AFM measurements. Such a 3D representation can be obtained fairly easily by triangulation of the depth map. Given the neighborhood relationships of the depth map, neighboring points are simply to be connected by triangles to create a surface approximation. Such a triangle mesh can then be displayed and examined under any viewing angle.

Far more interesting, but more difficult, is the building of complete 3D models of submicroscopic objects. Such generated 3D models offer new possibilities for the analysis of micro-objects by visualization or measurement in 3D space. The difficulty arises because only part of the object is visible on a given image or view. Thus, there is a need to collect and combine several views from the whole object surface in order to create a complete virtual model.

This view assembling is solved for macroscopic objects, i. e. [5, 7, 8], but the solutions do not directly apply to micro-object. Three main problems have to be handled in the case of 3D models building: view digitizing, view positioning, view fusion.

View digitizing requires to move either the sensor or the object to obtain the different views. This is easily performed in the case of macroscopic objects, when either the object or the sensor can easily be manipulated and moved around. Conversely, the case of microscopic objects is more complicated. Several potential methods can be considered. One can move the object

---

[*] Correspondence: Email: timothee.jost@imt.unine.ch; WWW: http://www-imt.unine.ch; Telephone: +41 32 7183459; Fax: +41 32 7183402

by using some vibration or by handling it with a physical device like the AFM tip itself. In the case of multiple occurrences of a same object, one can also try to extract the different views from different occurrences. All these methods just provide random positioning, as the view positions relative to the object are not known.

View positioning requires to establish the position of each view relative to the object. For macro-object, positioning is usually simple and results directly from the acquisition devices. For micro-objects however, as mentioned above, acquisition methods cannot provide a priori positioning information. To remedy this drawback, the idea developed in this paper is to solve view positioning by an a posteriori registration procedure that aligns views by registering common overlapping parts. The proposed positioning approach relies on the sole geometric properties of the object. The actual view registration process is a two step process: a first rough interactive alignment, followed by an automatic surface matching of the different views.

Finally, when views are correctly aligned, view fusion proceeds by merging the different triangle meshes into a unique surface for the 3D model.

The goal of this work is to assess the feasibility of acquiring and registering the surface geometry of micro-objects measured under different orientations with an AFM. Experiments concern the modeling of small quartz particles about 1-3 µm in size, out of a set of views covering the whole object. The perspective is to end up with the capability to fully reconstruct micro or nano objects from various AFM images.

A basic description of the modeling system can be found in section 2. Further sections focus on the description of view digitizing, view registration and view fusion, with an emphasis on micro-objects measurements. Finally, first results are presented and discussed.

2. SYSTEM ARCHITECTURE

A general diagram of the modeling system is presented in figure 1. Of course, the input of the system is the object to be scanned. Two main blocks are defined: view digitizing and view integration. The view digitizing block produces a virtual view for each different position of the micro-object. These virtual views are then combined in the view integration block, which outputs the expected complete virtual 3D model. A more detailed description of both blocks follows.

The main goal of view digitizing is to acquire the 3D data for each view and to present them in a virtual view format that preserves the topology of the scanned surfaces. Three main parts compose the view digitizing block: data acquisition consists in measuring the 3D geometry, in the present case by using an AFM. During data processing, geometric data can be filtered to remove noise and missing points, as well as to extract the considered object surface from the whole surface measurement. Finally, in view triangulation, the measured surface points are triangulated to create an adequate mesh representation of the surface.

The integration process is iterative, a new virtual view being added to the virtual model under construction at each step. The whole object modeling process starts with an empty virtual model and the digitizing of a first view. The first view integration step is trivial as the virtual model simply becomes the first view. Then the iterative construction process really starts and new object views are added successively to the growing virtual model until it is complete.

The view integration block is subdivided into another two blocks: view registration and view fusion. During view registration, the relative positioning between the new view and the virtual model is found. During view fusion, the new view and the virtual model are fused into a description that consists in single mesh.
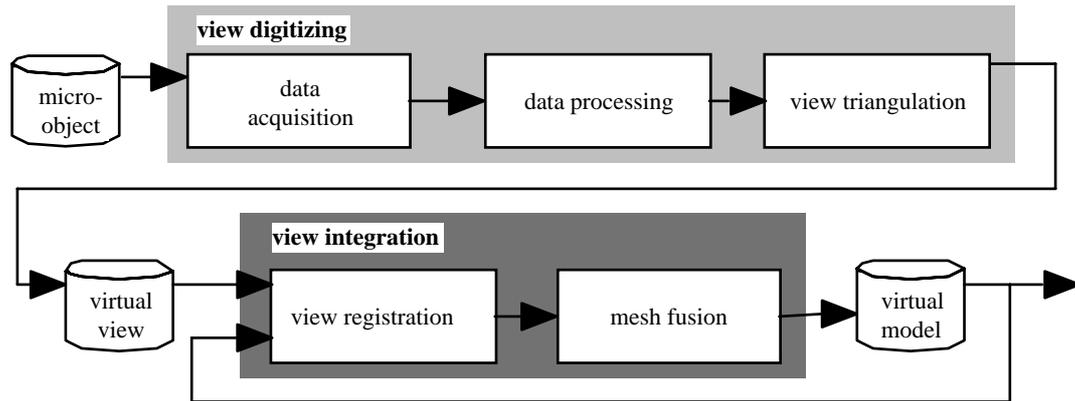
Figure 1. modeling system

Both view digitizing and view integration blocks are described and discussed in detail in the following sections.

3. VIEW DIGITIZING

3.1 Data Acquisition

In order to obtain a set of views covering its whole surface, the micro-object must be sensed under different orientation. Several potential method can be considered, depending on the type of sensor and the characteristics of measured object(s). One can move the object thanks to vibrations or some kind of handling. Moving the sensor around the object is generally not a possible solution in the case of micro-objects because of size and material constraints. Finally, in the case of multiple occurrences of the same object, one can try to extract the different views from different occurrences.

In our case, two solutions have been considered. The first one consists in using the AFM tip to move the particle. The AFM can work in static (contact) or dynamic (tapping) mode. Experiments showed that the lateral tip-to-sample interaction is too important and causes the particles to be moved around the substrate. This effect can be used to our advantage when it comes to moving the particles to get a new view. The second solution considers particles that have contaminated the tip. Experiments also showed indeed that particles could settle down on the tip, contaminating it. In that case, one can use a calibration tip sample to reverse-image the measurement: since the curvature of the calibration tips is much smaller than the one of the particle that contaminates the AFM tip, the particle itself will be imaged when scanning over the calibration tips. The static mode could also be used to slightly move the particle around the tip. Further details about data acquisition with the considered system can be found in [3].

3.2 Data Processing

Most of the techniques existing for the measurement of micro and nano surfaces, like the AFM, provide raw data in the form of a depth map. It consists of a bidimensional array of height z measurements defined at various discrete x, y positions. Such a depth map can be represented as a range image that uses a gray-level or pseudo color representation for the different z values. An example of a range image of a quartz particle can be observed in figure 2.a.

Data processing mainly consists in the filtering of the geometric data to remove noise and missing points. In the case of AFM measurements, there is an additional need to extract the considered object surface from its surroundings. This can generally be achieved by a simple z-value thresholding, to eliminate the unnecessary "background".
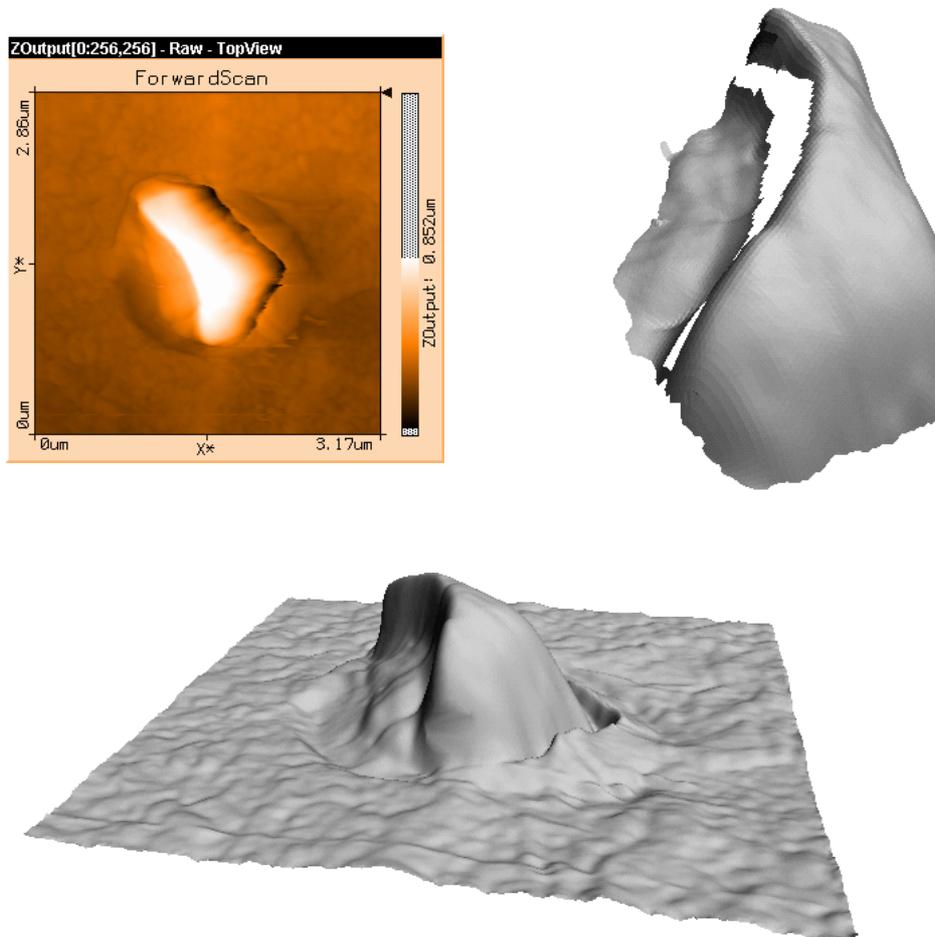
Figure 2. measurement of a quartz particle: (a) range image (b) triangulated surface (c) extracted triangulated view

3.3 View Triangulation

After data processing, the measured surface points are triangulated. Since the measurements are ordered in a regular grid, namely the depth map, the triangulation of the surface becomes straightforward as proposed by Rutishauser [4]. The depth map is traced from the upper left to the lower right corner and a local triangulation is performed for every pixel. The local triangulation algorithm creates two triangles covering the square grid mesh formed by the points $P_{i,j}$, $P_{i+1,j}$, $P_{i,j+1}$ and $P_{i+1,j+1}$ where i and j are the row and column indices of the current position in the range image. If the four points represent valid data, there exist two possible ways to triangulate the grid depending on which diagonal is selected. Following the principle of the Delaunay triangulation, the shortest diagonal is selected, which also creates triangles with a maximal size of the smallest angle. Since there are no triangles with long edges, it results in a smooth surface approximation. If one of the four points is not valid then one triangle is constructed with the remaining three points and no triangle is build at all if more than one point is missing.

For several applications, the full depth map resolution is not necessary and a subsampling of the rows and columns by a factor r allows to reduce the number of points and to process the data faster. This data reduction can be done easily by increasing the local triangulation mesh by a factor r, typically equal to 2 or 4. Figure 2b shows the triangulated representation of the range image 2a.

Note that checking the validity of the range points is not sufficient to avoid bad triangles. Other authors [5, 8] showed that additional checks are necessary to avoid the connection of range points separated by a discontinuity step in the range image.

Points which are next to one another in the range image are not necessarily neighbors on the object surface as illustrated by fig. 3.
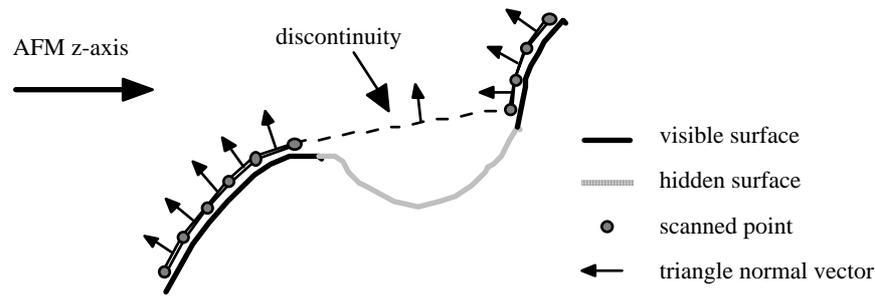

Figure 3. triangle size and orientation check

Therefore, there is a need to ensure that occluded parts are not covered by triangles. The procedure has two steps. First, only triangles with edges smaller than 4·s·r are kept, where s is the x, y sampling grid distance and r the reduction factor introduced before. Second, triangles which angle between the triangle normal vector and z axis exceeds 75° are rejected. Figure 2c shows the extracted triangulated view of the quartz particle.

4. VIEW INTEGRATION

Any additional view which is to be added to the virtual model has to be first registered and then fused with the virtual model.

4.1. View Registration

View registration aligns two 3D meshes. It only relies on the object surface characteristics. This assumes that the virtual model and the new object view have at least some common surface parts which allow to establish correspondences between them.

Even assisted by a sophisticated object rendering and pose manipulation hardware, an operator cannot align the meshes precisely. He would have to inspect the two surfaces again and again from different point of views and it is known that it is not easy at all to control the six degree of freedoms for fine pose tuning. On the other hand, automatic matching algorithms need a good starting configuration to converge successfully. Thus, one can separate registration in two distinct actions: rough positioning and fine positioning; rough positioning being solved by an interactive pose estimation task and fine positioning being solved by an automatic matching task.

Interactive pose estimation

Human perception easily identifies corresponding surface parts for any object type and shape. Therefore, the user can easily enter a hint for the computer which will then calculate the precise alignment using the automatic matching algorithm described in the next section. The system provides an interactive interface that permits an operator to enter a pose estimate for the two objects to be aligned. Both the virtual model and the new view are rendered in 3D and can be manipulated in all six degree of freedoms using a space mouse as input device. Figure 4 shows an example of two roughly aligned surfaces used as starting configuration for the automatic matching.
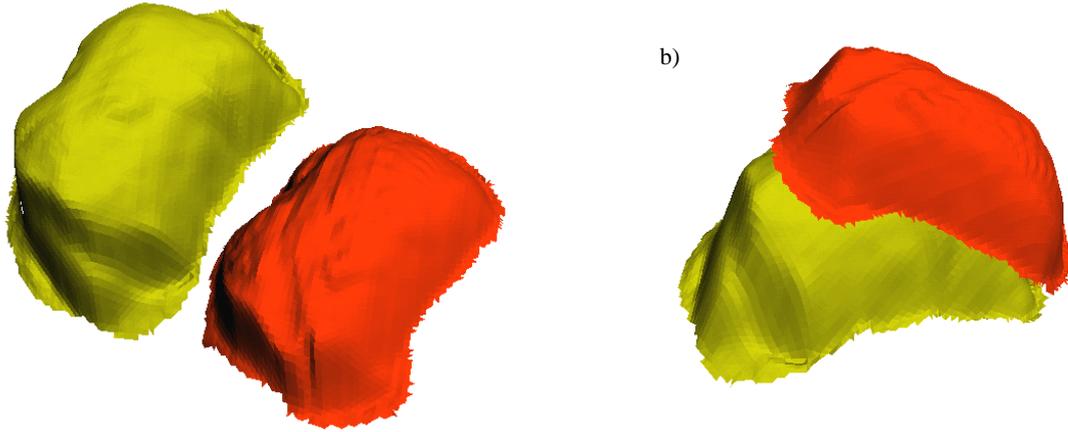
Figure 4. (a) two views of a quartz particle (b) roughly aligned views

Automatic matching

A variation of the iterative closest point algorithm [1] (ICP) is used for performing automatic surface registration. This algorithm registers two surfaces starting from an initial pose estimate. It proceeds iteratively. First, it pairs every point of one surface called P with the closest point of an other surface called X. These pairs of closest points are used to calculate the rigid transformation (**R**, **t**), which minimizes their mean square coupling distance or error *e*. The surface P is then translated and rotated by the resulting transformation and the algorithm starts again with the closest point coupling. This algorithm has been shown to converge but not necessarily towards the optimal solution. A good starting configuration is preliminary to a successful convergence. However, the range of successful starting configurations is rather large (see [4] and fig. 4) and does not constraint the operator too much when entering a pose estimate.

In the original algorithm one surface is a subpart of the other which is not the case in our application where each surface contains data not present in the other. The ICP algorithm needs therefore to be modified [8] : closest points which are too far apart are not considered to be corresponding points and are not coupled. This modification assigns the weight zero to invalid couplings as shown in figure 5.
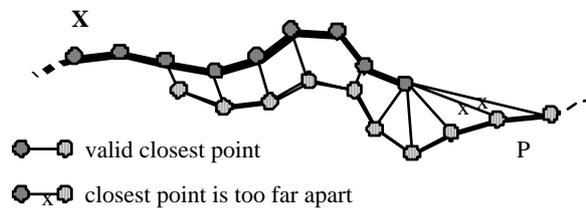

Figure 5. closest point couplings for two surfaces

The considered registration algorithm also integrates surface orientation in the computation of distance for the closest point computation [6]. It permits to have a better coupling, especially when two close surfaces possess different orientations.

The four steps of the algorithm can be summarized as follows:

given $\mathbf{x}_k \in X$ and $\mathbf{p}_k \in P$,

1) Compute closest points by means of the distance function d: $\forall \mathbf{p}_k \in P$, find $\mathbf{x}_k = \min\left[d(\mathbf{p}_k, X)\right]$

2) Define weight couplings:
$$w_k = \begin{cases} 1 & d(\mathbf{p_k}, \mathbf{x_k}) < d_{thres} \\ 0 & else \end{cases}$$
$$k \in [1, \ldots, N_p]$$

3) Compute best transformation: minimize $e(\mathbf{R}, \mathbf{t}) = \dfrac{1}{W} \sum_{N_p} w_k \|\mathbf{R}\mathbf{p_k} + \mathbf{t} - \mathbf{x_k}\|^2$, $W = \sum_{N_p} w_k$

4) Apply the geometric rigid transformation: apply ($\mathbf{R}$, $\mathbf{t}$) to P

The iteration stops when the change in the coupling error at iteration i falls below a threshold: $e_{i-1} - e_i < \tau$

Experience shows that this modified ICP algorithm converges quickly. As mentioned before, the two surfaces should have enough common data points. 30 to 50 % of common surface has been observed to be a good amount. The common surfaces also have to possess enough characteristics to match correctly: two sphere parts or planes won't match correctly because of the lack of local characteristics! Figure 6 shows the same surfaces as in figure 4 after the execution of the automatic matching.
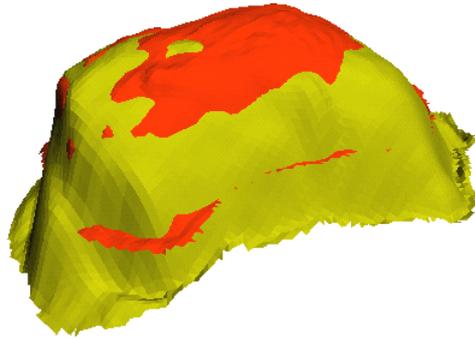

Figure 6. fully registered surfaces

4.2. View Fusion

Once the surfaces are matched, they must be fused together in order to eliminate redundant data and to create a unique mesh. The different methods used to fuse 3D views can be separated into two groups: partial erosion of surfaces and complete retriangulation of the surface points. First methods [7, 8] erode the overlapping surfaces until the overlap disappears. The two surface meshes are then recombined at their frontiers in order to have one unique mesh for the union of the two surfaces. Second ones [5] discard the mesh information from the triangulated views, if calculated at all, and retriangulate the overlapping zone or even the complete point set.

The view fusion algorithm considered here belongs to the first group. It operates on triangle meshes and proceeds by erosion. It takes advantage of the correspondence established during registration to eliminate redundant surfaces and to triangulate the resulting gap. More precisely, this mesh fusion algorithm is characterized by the following steps:

1) **overlap detection**: The valid couplings from the previous automatic matching are used to easily identify the parts of surface P which overlap surface X where P and X are defined as in the previous section.

2) **overlap erosion**: The overlap part of surface P is eroded.

3) **frontier detection**: A gap separates the surface X and the eroded surface P. The frontier on P is calculated during the overlap erosion where a closest point search detects the start of the frontier on X.

4) **gap filling**: The gap enclosed by the two frontiers is filled with triangles. The filling algorithm works in 3D space and does not need any projections into tangential planes which increases its reliability.

The algorithm is presented in details and discussed in [7].

5. EXPERIMENTS

All investigations were done with an experimental modeling software and hardware. Data acquisition is performed by an AFM described in [2]. It delivers generally 256x256 depth maps with a xy ranges varying typically between 20 nm and 50 µm and a z range of up to 3 µm. The modeling software works on a SGI Indigo2 Impact workstation and is programmed with the Open Inventor library in c++. It permits to process all the steps of the modeling, from the processing of the raw depth map to registration and fusion of the views. The software interface can be seen in figure 9.

Figure 7 presents the range image and triangulated view of a rectangular and flat calibration grid. These two representations permit to see the distortions that appears with uncalibrated measures. The x and y distortions can clearly be seen in the range image. The z values have been increased by a factor 5 in the triangulated view. It permits to have a better idea of the z distortion. Small distortions are not critical as long as only a single view is taken into account for representation purpose. On the other hand, there is a need for calibration of the AFM in the case of 3D object modeling because distortions on the different views create problems in both registration and fusion processes.
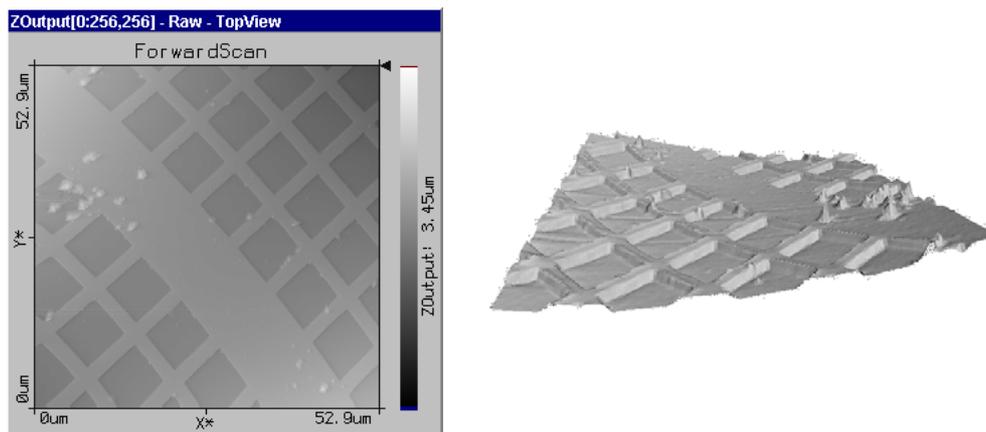

Figure 7. distortion of measurement seen in the range image and triangulated view of a calibration grid

First experiments consisted in measuring the substrates and the loose quartz particles poured onto it. Figure 8 presents 2 triangulated views of the same quartz particle, measuring about 1.5 µm. Both views have been taken by reverse-imaging a particle contaminating the AFM tip. One can note here that tip contamination by particles has been showed to happen quite frequently experimentally. The difference between both views is that the calibration tip sample has been turned 45° around the z axis. Both extracted triangulated views of the quartz particle have then been registered (figure 4 and 6). The registration result shows that the second view is smaller of roughly 2% and contains noticeable distortion. These differences come from the fact that the tip of the calibration sample has a certain structure that is not perfectly symmetric around the z axis. This should also be taken into account to get rid of the resulting distortions.
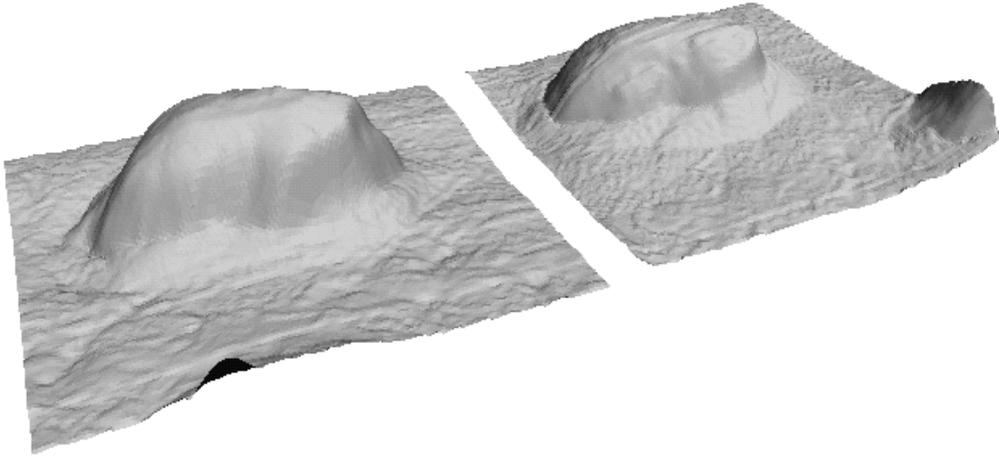
Figure 8. two triangulated surfaces of the same quartz particle at same orientation, taken by reverse-imaging

Finally, to test the principle of view integration, we tried to take different views of the same surface with just an offset in xy, keeping the same orientation. Figure 9 represents the a range image of the measurement of Ni-polymer substrate. Its size is approximately 50x50 µm. The 3 highlighted parts of the surface (15x15 µm) have been measured individually and the resulting data have been introduced into our modeling software. The successful result of the integration of the three views is also shown into the software environment.
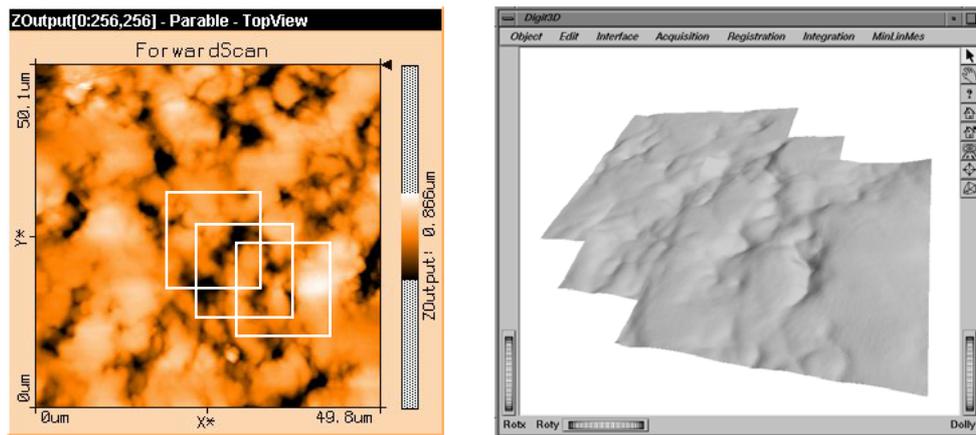

Figure 9. three views of a Ni-polymer substrate successfully integrated, shown in the modeling software interface

6. CONCLUSION

Building 3D virtual models of microscopic objects offers new possibilities for their analysis by visualization or measurement. The experimental system presented is expected to create 3D models by integrating several AFM measurements of the considered object observed under different orientations. As the relative positioning of the different views is not known in the case of AFM measurements - due to the random aspect of the orientation change between the different views - the presented approach proposes to use an a posteriori software registration procedure that aligns views by registering common overlapping parts. It relies on the sole intrinsic properties of the object geometry and does not require additional measurements.

First experiments have been made with the considered system. They consisted in measuring loose quartz particles poured onto a substrate. Several single views from different particles have been obtained in both normal and reverse-image mode. Results showed that calibration of the AFM is required in order to obtain views that can be correctly matched. Finally, three views of the substrate have been integrated together successfully.

Further work towards building a full 3D model of a particle includes more testing to move the particles around (moving them with the AFM tip seems promising but potential problem exist with contamination) and calibration of the reverse-image mode, as well as investigations towards a better understanding of the underlying mechanisms.

ACKNOWLEDGEMENTS

REFERENCES

1. P.J. Besl and N.D. McKay, "A Method for Registration of 3-D Shapes," *Proceedings of IEEE Transactions on Pattern Analysis and Machine Intelligence (PAMI),* vol. 14(2), pp. 239-256, 1992.

2. S. Gautsch, T. Akiyama, H. R. Hidber, L. Howald, D. Muller, P. Niedermann, W. T. Pike, N. F. de Rooij, U. Staufer, A. Tonin, "Development of an AFM Microsystem for Nanoscience in Interplanetary Research*", Third round table on micro-nanotechnologies for space*, vol. 174, pp. 173-177, Noordwijk, The Netherlands, 2000.

3. S. Gautsch, T. Akiyama, R. Imer, N. F. de Rooij, U. Staufer, P. Niedermann, L. Howald, D. Brändlin, A. Tonin, H. R. Hidber, W. T. Pike, "Measurement of Quartz Particles by Means of an Atomic Force Microscope for Planetary Exploration", *To be published in Proceedings of SXM-4 Conference,* Muenster, Germany, 2000.

4. H. Hügli, Ch. Schütz, "How Well Performs Free-Form 3D Object Recognition from Range Images," *Intelligent Robots and Computer Vision XV, Algorithms, Techniques, Active Vision and Materials Handling*, SPIE, 2904, pp. 66-74, Boston, 1996.

5. M. Rutishauser, M. Stricker, M. Trobina, "Merging Range Images of Arbitrarily Shaped Objects," *Proceedings of the IEEE Conference on Computer Vision and Pattern Recognition (CVRP),* pp. 573-580, Seattle, 1994.

6. C. Schütz, T. Jost, H Hügli, "Multi-Feature Matching Algorithm for Free-Form 3D Surface Registration", *14th International Conference on Pattern Recognition, ICPR'98*, vol. 2, pp. 982-984, IEEE Computer Society, Brisbane, 1998.

7. C. Schütz, T. Jost, H. Hügli, "Semi-Automatic 3D Object Digitizing System Using Range Images*", Proceedings Asian Conference on Computer Vision, ACCV'98*, vol. 1, pp. 490-497, Hong Kong, 1998.

8. G. Turk, M. Levoy, "Zippered Polygon Meshes from Range Images," *Proceedings ACM Siggraph '94*, pp. 311-318, Orlando, 1994.